

FORC study of the ferromagnetic impurities in Na and K feldspars of “El Realejo” mine

Cite as: AIP Advances 9, 035038 (2019); doi: 10.1063/1.5080081
Presented: 15 January 2019 • Submitted: 5 November 2018 •
Accepted: 15 February 2019 • Published Online: 21 March 2019



Jose Antonio Montiel-Anaya  and Victorino Franco^{a)} 

AFFILIATIONS

Dpto. Física de la Materia Condensada, ICMSE-CSIC, Universidad de Sevilla, Apdo. 1065, 41080 Sevilla, Spain

Note: This paper was presented at the 2019 Joint MMM-Intermag Conference.

^{a)} **Corresponding author:** Victorino Franco. Email: vfranco@us.es

ABSTRACT

Feldspar is a Na-K-Ca-Al tectosilicate, generally poor in iron or other elements with large magnetic moments. Being the most abundant constituent minerals in Earth's crust, feldspars are technologically used in a broad variety of applications, which include glass-manufacturing, fabrication of ceramics elements, fillers in paintings, enamels, floors, etc. However, most applications require the absence (or minimization) of Fe inclusions, being this a very relevant factor that controls the price of the mineral. Typically, Fe content in the mineral produced at a mine is determined by chemical analysis, which implies an off-site test and small sampling volume. Separation of magnetic inclusions is usually made by crushing the rocks and applying a magnetic field gradient that, in combination with gravity, guides the magnetic particles out from the production line. In this work we use FORC to determine the content of the magnetic phases and show that the conventional separation methods used in the mine, which indirectly affect the final price of the product, are selective in the extraction of magnetic particles, as evidenced by the different FORC distribution of the natural rock and that of the separated particles.

© 2019 Author(s). All article content, except where otherwise noted, is licensed under a Creative Commons Attribution (CC BY) license (<http://creativecommons.org/licenses/by/4.0/>). <https://doi.org/10.1063/1.5080081>

I. INTRODUCTION

Natural samples respond in some way to magnetic fields. Some minerals have diverse magnetic properties and are sensitive to magnetic field of earth¹ and environmental processes. The classification of magnetic components inside natural samples is important in order to assign their nature and origin (rock forming processes) and can provide, for example, climatic and diagenetic signals. In addition, from the point of view of the mining industry, the application of magnetic characterization could be interesting in order to improve the separation techniques of these magnetic phases from the ore in the treatment phase of the mineral.

We have studied alkali feldspar from “El Realejo” mine located in Sevilla, Spain. The production of “El Realejo” mine has represented the 25% of the national production in Spain for 10 years. However, there is little knowledge about which magnetic phases are present inside this feldspar production, as Fe content is usually determined by chemical analysis. Improving the techniques used nowadays for magnetic characterization and separation of these particles would lead to an eventual improvement of the final product.

Feldspars from “El Realejo” mine have an igneous origin. Magnetic minerals are formed by crystallization within igneous rocks while they cool down. Once igneous rocks come in contact with external agents like water or air, they start to undergo weathering. Magnetic characterization is an efficient tool for characterizing such changes of Fe²⁺ or Fe³⁺ ions held in iron oxides (magnetite, maghemite, hematite) and iron oxyhydroxides (goethite, ferrihydrite).²

In this paper, we study the ability of First Order Reversal Curves (FORC) distributions to unravel complex magnetic signals, as bimodal distributions and mixtures of different magnetic phases in natural alkali feldspar samples and to gain insight about the results of the separation processes used in the mine.

II. METHODS

A. Sample preparation

K- and Na-feldspar stones from “El Realejo” mine in Cazalla de la Sierra were selected, since these two types are the most industrially representative from this mine. A virtual visit to

the site from where samples were extracted can be seen through this link.³

Some representative fragments were selected to obtain the natural samples K-feldspar and Na-feldspar, with an approximate diameter of 5 mm that would allow us to perform the magnetic characterization in a Vibrating Sample Magnetometer (VSM).

Samples Kfeldspar_ext and Nafeldspar_ext were crushed from massive K-feldspar and Na-feldspar aggregates, respectively, and consist of the particles separated magnetically from the rest.

B. Magnetic measurements

Magnetic hysteresis loops, remanent curves (isothermal remanent magnetization and DC demagnetization) and FORC measurements were measured using a Lake Shore Cryotronics 7407 VSM at room temperature.

The maximum applied field was 1.5 T; lower values were used as acceptable for softer magnetic samples. 1.5 T would not be enough to completely saturate common minerals like goethite with high switching field, which could be unsaturated at fields larger than 57 T.⁴ Nevertheless, the maximum applied field is much larger than the coercivity of the current samples, making them be in the technical saturation region. It is important to understand the behavior of these minerals using standard equipment, as this would allow comparison among different results.⁵

Remanent magnetization (M_r), saturation magnetization (M_s) and coercive field (H_c) were determined from hysteresis loops measured with a maximum applied field of 1.5 T, after removing the paramagnetic linear contribution of the sample by linear fitting the high field slope of the loops (Figure 2). IRM and DCD remanence curves were calculated with a stepwise procedure with 150 steps and a maximum field of 1T. From them, the remanent coercive field (H_{cr}) at room temperature was determined.

For all samples, FORC (first order reversal curves) characterization was performed at room temperature with the VSM. A FORC diagram is calculated from minor hysteresis curves, called FORCs.⁶ First, one FORC is acquired saturating magnetically the sample by applying a positive external magnetic field. Secondly, a backfield is applied to a reversal field H_a ; then the applied field is increased up to saturation again applying field steps H_b . A FORC is the magnetization curve from H_a to $H_{saturation}$, measured at field values H_b . Finally, several FORCs are measured with different reversal fields H_a to obtain a magnetization grid necessary to build a FORC distribution diagram calculated through the second mix derivate⁷ (equation 1):

$$\rho(H_b, H_a) = -\frac{1}{2} \frac{\partial^2 M(H_a, H_b)}{\partial H_a \partial H_b} \quad (1)$$

Where $M(H_a, H_b)$, is the magnetization of any field H_b within the curve of reversal field H_a . To expedite the analysis, usually a change of coordinates is performed:

$$\begin{aligned} H_c &= (H_b - H_a)/2 \\ H_u &= (H_b + H_a)/2 \end{aligned} \quad (2)$$

FORC diagrams provide a map of the magnetic response of our natural samples in terms of coercivity H_c and interaction magnetic field H_u distribution.⁸

For each sample, 200 FORCs were performed at room temperature with a saturation field up to 1.5 T, averaging time of 100 ms and average field increment of 10 mT between consecutive measurements. FORC diagrams were processed with the FORCinel software,^{9,10} version 3.03. The optimum smooth factor was explored, starting with 1 and finishing with 10 (the smooth factor increment was 1 and the output resolution factor was 3). The smooth factor used for the presented distributions was 7.

C. XRD analysis

For all samples, their phases were characterized using X-ray diffraction (Bruker D8 Advance diffractometer with Cu K α radiation).

III. RESULTS AND DISCUSSION

From X-ray diffractograms of the K-feldspar samples (Fig. 1a), where only the magnetic phases have been marked, we can observe the coexistence of magnetite, hematite and goethite phases.

For the Na-feldspar samples (Fig. 1b), the diffractograms show the occurrence of two phases: magnetite and goethite. Magnetite is a magnetically softer phase, with a high spontaneous magnetization, while goethite is harder and has a weaker spontaneous magnetization.

Figure 2 shows the hysteresis loops of K-feldspar and Na-feldspar samples, together with the deconvolution of the linear part corresponding to the paramagnetic fraction of the samples. Hysteresis parameter are summarized in Table I. The K-feldspar samples show wasp-waisted shape,^{11-13,7} which could be explained by the existence of several uncoupled phases with different coercivities. These samples are also magnetically harder than Na-feldspar samples, which could indicate the plausible presence of harder phases like hematite or goethite. K-feldspar also exhibits weaker magnetization (Table I). However, wasp-waisted shape could also be explained by particle size heterogeneity. The Na-feldspar samples are magnetically soft (Table I) and have larger magnetization. They do not show wasp-waisted shape, which indicate a likely presence of one soft magnetic phase.

IRM-DC demagnetization (Figure 3) shape analysis of K-feldspar seems to reach a plateau for low fields. However, if the applied field is increased, remanent magnetization continues to grow up until values close to saturation field. This could be explained by the presence of several magnetic phases with different coercivities. Na-feldspar samples do not show this two stages shape and reach saturation with lower applied fields. The observed smaller H_{cr} in extracted feldspars samples compared to the natural samples could be caused by the loss of magnetic particles during the extraction separation stage.

FORC diagrams for K-feldspar samples are shown in Figure 4(a) and (c). All the samples analysed are at or close to magnetic saturation at 1.5 T (15 kOe) (Figure 2). In the FORC diagram for K-feldspar samples we can clearly distinguish two switching field distribution peaks, indicating the presence of at least two uncoupled phases. The first one has a distinct peak near $H_c=0$ and this distribution spreads along the H_u axis, This first coercivity peak is associated with particle with multidomain behaviour (MD).⁷ The inclined contours that intersect with H_u axis likely result from

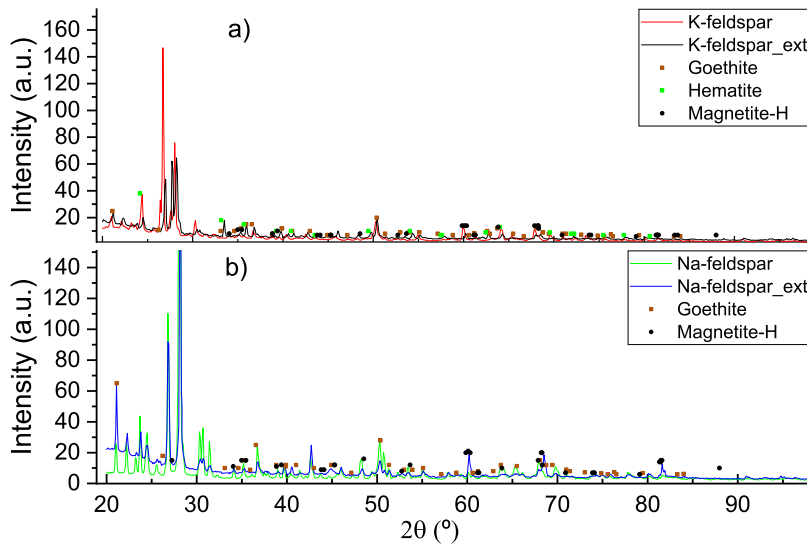


FIG. 1. X-ray diffractograms for K-feldspar samples (a) and Na-feldspar samples (b). The green, brown and black dots represent characteristic reflections for hematite, goethite and magnetite respectively.

magnetic interactions among domain walls.^{14,15} The higher coercivity peak has an asymmetric closed structure, indicating single domain behaviour (SD), with a maximum at $H_c \sim 4250$ Oe (425mT). The full width at half maximum (FWHM) of the peak along the H_u axis gives a measure of the dipolar interaction field,¹⁶ which is ~ 500 Oe for this sample. Most of the contours of this peak lie below the H_c axis. This asymmetry could be caused by interactions among

particles.^{8,17} However, Roberts et.al.¹⁸ have shown that part of the asymmetry could be explained from the fact that the measurements start at positive saturation.¹⁸

The FORC diagram for the extracted K-feldspar (K-feldspar_ext), Figure 4(c), is qualitatively similar to that of the natural K-feldspar. It also shows two coercivity peaks, although the second one has less intensity than in the natural sample

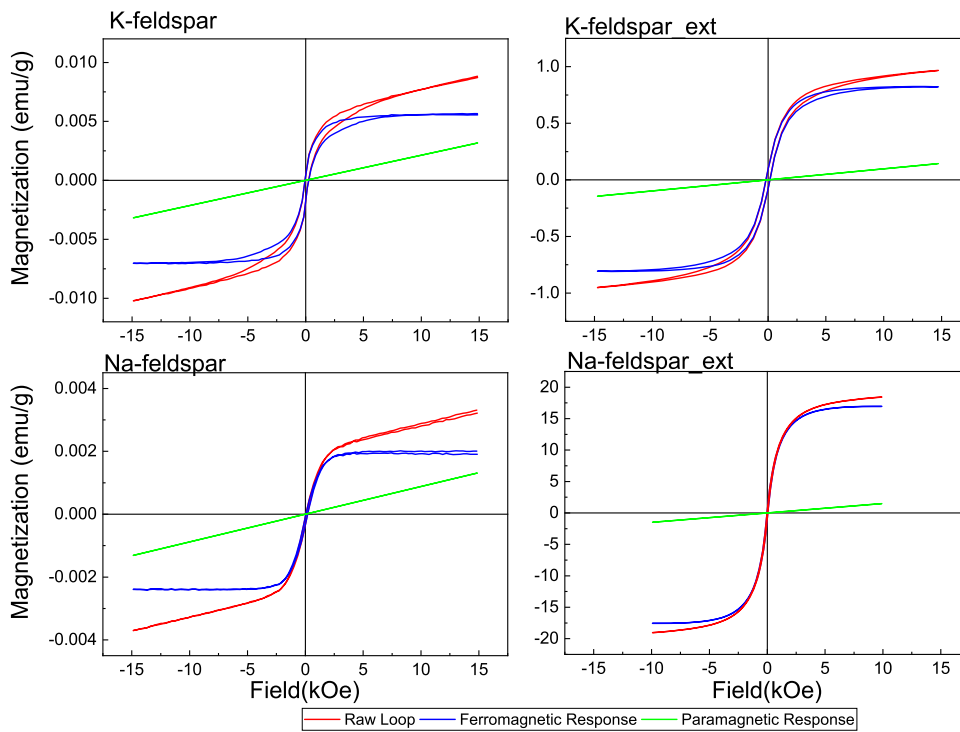


FIG. 2. Hysteresis loops measured at room temperature before (red -raw loop) and after (blue ferromagnetic response) high field slope correction, together with the corresponding paramagnetic signal (green) for all four samples.

TABLE I. Hysteresis parameters of the four samples: Saturation magnetization (M_s), remanent magnetization (M_r), coercive field (H_c), and remanent coercivity (H_{cr}).

Sample	Mass (mg)	H_c (Oe)	M_r (emu/g)	M_s (emu/g)	H_{cr} (Oe)
K-feldspar	467.632	156.7	1.08E-03	9.52E-03	2547.5
K-feldspar_ext	15.358	172.1	8.80E-02	9.59E-01	691.9
Na-Feldspar	856.874	78.6	1.41E-04	3.51E-03	1563.4
Na-feldspar_ext	4.6153	35.4	6.63E-1	1.87E+01	62.2

(Figure 4(a)). This difference should be attributed to the process of extraction and separation of the magnetic phases from the rock to prepare the sample.

The first dominant peak near $H_c \sim 0$ could be associated with a soft magnetic phase like magnetite, or two coupled magnetic phases formed by soft magnetite with large M_s plus a harder phase but with weak saturation magnetization like hematite or goethite, as its magnetic signal would be muted by the phase with strong saturation magnetization.^{19,20} According to literature values, the second peak could be ascribed to goethite or hematite.^{7,19} It is known that natural samples of hematite or goethite are usually not pure. In the case of hematite, impurities are normally aluminous hematite ($\alpha\text{-Fe}_{2-x}\text{Al}_x\text{O}_3$) because Al substitution is very common in nature.² Furthermore, it is reported that hematite has a notable feature, which is increasing coercivity values with growing Al content, as reported Roberts et. al.⁵ In addition, the locations of these second peaks agree with the values reported by Carvallo et. al.¹⁹ and Muxworthy et.al.²¹ with a peak centred at large coercivity (around 400 mT), therefore the second peak with 425 mT of coercivity at the FORC diagrams could be associated to hematite. On the other hand, unlike for hematite, it is not easy to make

statements about the influence of Al substitution on FORC distribution for goethite.^{5,22} The higher second coercivity peak (425 mT) could also be caused by goethite according with Roberts et. al.⁷ and Dekkers et. al.²³

The FORC diagrams for Na-feldspars (Figure 4(b) and (d)) both show one main peak near $H_c \sim 0$ Oe with contours with some vertical spread that intersect the H_u axis. This is probably the result of magnetic interactions among domain walls,¹⁸ in agreement with the magnetic parameters obtained from the hysteresis loop: large magnetization and low coercivity.

Nevertheless, we can observe that at the last contours have higher coercivities of ~ 150 mT, with some elongation that indicate some interaction field distribution that could be caused by the presence of a second phase which is less detectable due to the presence of the phase with stronger magnetization (M_s). This is in agreement with the literature,¹⁹ where it is shown that FORC is able to detect phases with small magnetization like hematite or goethite mixed with another phase with stronger magnetization like magnetite, provided that the content of the high magnetization phase is less than 12%.^{19,24} The interpretation of the FORC diagrams and the corresponding magnetic phases agrees well with the results extracted from X-ray diffraction data presented above.

IRM and DC demagnetization curves provide information that can also be determined from the FORC characterization.¹⁸ Figure 3b–e show the coercivity distribution calculated from the first derivate of IRM curves, while Figure 4 shows the derivative of the backfield remanence curve that corresponds to the backfield coercivity distribution⁹ extracted from the FORC distributions. Both methods agree in that the K-feldspar samples have one low coercivity peak ($H_c \sim 0$) and another high coercivity peak ($H_c \sim 425$ mT). For the Na-feldspar samples the results only show a relevant peak near to $H_c \sim 0$. This confirms the good agreement between the results obtained from DCD/IRM and FORC analysis.

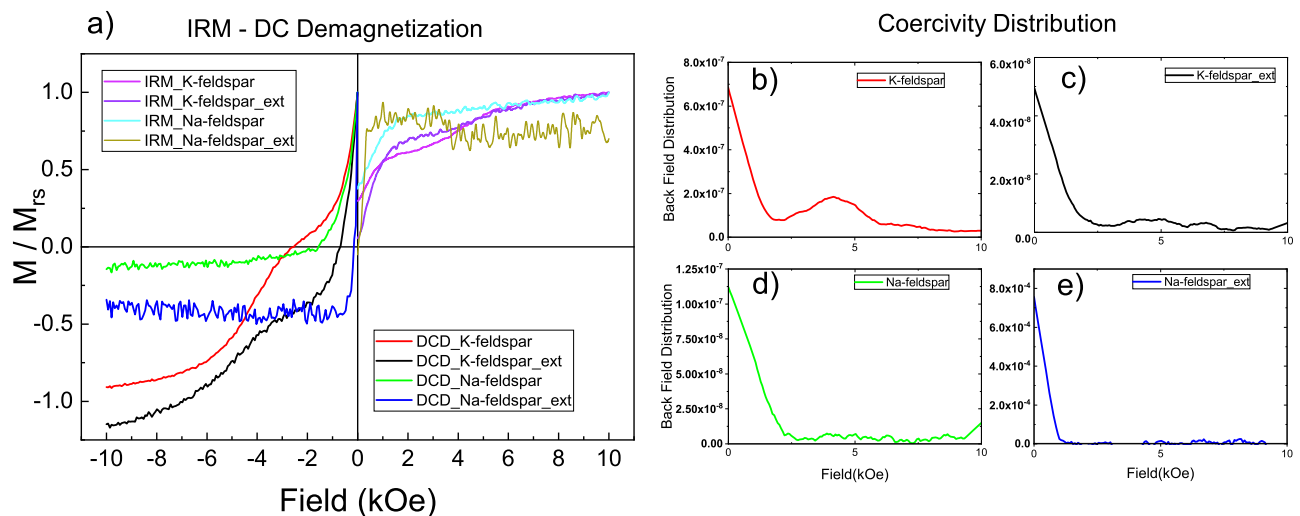


FIG. 3. (a) IRM (first quadrant) and DCD demagnetization (third and fourth quadrant) curves for Na-K- feldspar samples. (b-e) Coercivity distribution obtained from IRM and DC demagnetization curves.

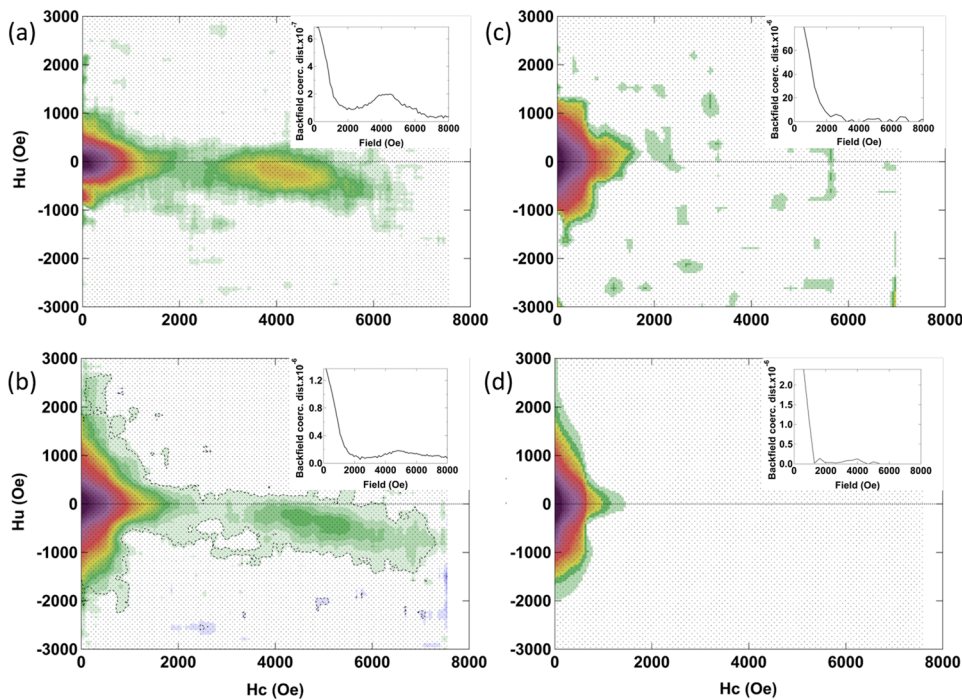


FIG. 4. FORC diagrams for K-feldspar (a, b) and Na-feldspar samples (c, d). a and c represent the natural samples while b and d correspond to the extracted samples. Colouring indicates the relative FORC contour density with blue corresponding to zero density and purple to maximum density. Insets: coercivity distribution obtained from FORC measurements.

It is worth stressing the differences between the distributions of natural and extracted K-feldspars samples, which also correlate well with the coercivity distributions presented in Figures 2 and 4. The decrease of the higher coercivity peak should be ascribed to a selective separation procedure that does not extract all the magnetic particles but mostly those with the smaller coercivities. As in the case of Na-feldspar we did not detect magnetically uncoupled high coercivity phases, there is no difference between distributions between natural and extracted phases. This selective separation might pose a relevant problem for the optimization of the final product of the mine, as the presence of the higher coercivity particles would imply a larger Fe content and, therefore, the unsuitability of the material for some technological applications.

IV. CONCLUSIONS

Feldspars are the most abundant minerals on earth and their applicability for some specific industries relies on the absence of Fe impurities. We have performed FORC analysis on natural samples from the “El Realejo” mine in Spain, and on samples of the extracted magnetic phases from the natural rocks. The interpretation of the results show the ability of FORC to discriminate uncoupled phases with different coercivities, even with hard and soft magnetic phases present in the natural sample. Therefore, FORC diagram is useful for both characterization and discrimination of the magnetic phases present in natural samples.

Microstructurally, X-ray diffraction shows at least three magnetic phases in K-feldspar and two phases in Na-feldspar samples, in agreement with the interpretation of FORC distributions.

FORC distributions are different for natural and extracted samples, indicating a selective character of the separation technique, which could have an influence of the final application of the material. The reliability of the magnetic analysis, which could be implemented near to the mining site, and its simpler character than off-site chemical analysis, could facilitate a more exhaustive characterization of the mining products and eventually facilitate its commercialization.

REFERENCES

- Z. Jiang, Q. Liu, M. J. Dekkers, V. Barron, J. Torrent, and A. P. Roberts, “Control of Earth-like magnetic fields on the transformation of ferrihydrite to hematite and goethite,” *Sci. Rep.* **6**(April), 1–11 (2016).
- M. E. Evans and F. Heller, “Environmental magnetism : Principles and applications of enviromagnetics,” 1–50, 2003.
- “Visita virtual a la mina ‘El Realejo’, Cazalla de la Sierra, Sevilla. <https://youtu.be/rvYir5Gpa7U>,” p. 7.
- P. Rochette *et al.*, “Non-saturation of the defect moment of goethite and fine-grained hematite up to 57 Teslas,” *Geophys. Res. Lett.* **32**(22), 1–4, <https://doi.org/10.1029/2005gl024196> (2005).
- A. P. Roberts *et al.*, “Characterization of hematite (α - Fe_2O_3), goethite (α - FeOOH), greigite (Fe_3S_4), and pyrrhotite (Fe_7S_8) using first-order reversal curve diagrams,” *J. Geophys. Res. Solid Earth* **111**(12), 1–16, <https://doi.org/10.1029/2006jb004715> (2006).
- I. D. Mayergoyz, “Mathematical models of hysteresis (Invited),” *IEEE Trans. Magn.* **22**(5), 603–608 (1986).
- A. P. Roberts, C. R. Pike, and K. L. Verosub, “First-order reversal curve diagrams: A new tool for characterizing the magnetic properties of natural samples,” *J. Geophys. Res. Solid Earth* **105**(B12), 28461–28475, <https://doi.org/10.1029/2000jb900326> (2000).
- C. R. Pike, A. P. Roberts, and K. L. Verosub, “Characterizing interactions in fine magnetic particle systems using first order reversal curves,” *J. Appl. Phys.* **85**(9), 6660–6667 (1999).

- ⁹R. J. Harrison and J. M. Feinberg, "FORCinel: An improved algorithm for calculating first-order reversal curve distributions using locally weighted regression smoothing," *Geochemistry, Geophys. Geosystems* **9**(5), n/a, <https://doi.org/10.1029/2008gc001987> (2008).
- ¹⁰R. Egli, "VARIFORC: An optimized protocol for calculating non-regular first-order reversal curve (FORC) diagrams," *Glob. Planet. Change* **110**, 302–320 (2013).
- ¹¹A. P. Roberts, Y. Cui, and K. L. Verosub, "Wasp-waisted hysteresis loops: Mineral magnetic characteristics and discrimination of components in mixed magnetic systems," *J. Geophys. Res.* **100**(B9), 17909–17924, <https://doi.org/10.1029/95jb00672> (1995).
- ¹²L. Tauxe, T. A. T. Mullender, and T. Pick, "Potbellies, wasp-waists, and superparamagnetism in magnetic hysteresis," *J. Geophys. Res. Solid Earth* **101**(B1), 571–583, <https://doi.org/10.1029/95jb03041> (1996).
- ¹³J. E. T. Channell and C. McCabe, "Comparison of magnetic hysteresis parameters of unremagnetized and remagnetized limestones," *J. Geophys. Res. Solid Earth* **99**(B3), 4613–4623, <https://doi.org/10.1029/93jb02578> (1994).
- ¹⁴D. J. Dunlop and Ö. Özdemir, "Magnetizations in rocks and minerals," *Treatise on Geophysics* (Elsevier, 2015), pp. 255–308.
- ¹⁵D. J. Dunlop, M. F. Westcott-lewis, and M. E. Bailey, "Preisach diagrams and anhysteresis: Do they measure interactions?," **65** (1990).
- ¹⁶C. Carvallo *et al.*, "Increasing the efficiency of paleointensity analyses by selection of samples using first-order reversal curve diagrams," *J. Geophys. Res. Solid Earth* **111**(12), 1–15, <https://doi.org/10.1029/2005jb004126> (2006).
- ¹⁷A. Stancu, C. Pike, L. Stoleriu, P. Postolache, and D. Cimpoesu, "Micromagnetic and Preisach analysis of the first order reversal curves (FORC) diagram," *J. Appl. Phys.* **93**, 6620–6622 (2003).
- ¹⁸A. P. Roberts, D. Heslop, X. Zhao, and C. R. Pike, "Understanding fine magnetic particle systems through use of first-order reversal curve diagrams," *Rev. Geophys.* **52**(May), 77–117 (2013).
- ¹⁹C. Carvallo, A. R. Muxworthy, and D. J. Dunlop, "First-order reversal curve (FORC) diagrams of magnetic mixtures: Micromagnetic models and measurements," *Phys. Earth Planet. Inter.* **154**(3–4), 308–322 (2006).
- ²⁰A. R. Muxworthy, A. P. Roberts, A. R. Muxworthy, and A. P. Roberts, "First-order reversal curve (FORC) diagrams," In D. Gubbins and E. Herrero-Bervera, editor, *Encyclopedia of Geomagnetism and Paleomagnetism*, Springer, 2007, Pages 266–272, *Encycl. Geomagn. Paleomagn.*, 266–272, 2007.
- ²¹A. Muxworthy and W. Williams, "Magnetostatic interaction fields in first-order-reversal-curve diagrams," *J. Appl. Phys.* **97**, 063905 (2005).
- ²²Q. Liu, Y. Yu, J. Torrent, A. P. Roberts, Y. Pan, and R. Zhu, "Characteristic low-temperature magnetic properties of aluminous goethite [α-(Fe, Al)OOH] explained," *J. Geophys. Res. Solid Earth* **111**(12), 1–12, <https://doi.org/10.1029/2006jb004560> (2006).
- ²³M. J. Dekkers, "Magnetic properties of natural goethite-I. Grain size dependence some low- and high-field related rockmagnetic parameters measured at room temperature," *Geophys. J. Int.* **97**, 323–340 (1989).
- ²⁴M. Ahmadzadeh, C. Romero, and J. McCloy, "Magnetic analysis of commercial hematite, magnetite, and their mixtures," *AIP Adv.* **8**, 056807 (2018).